

Discrete Polyphase Matched Filtering-based Soft Timing Estimation for Mobile Wireless Systems

Thomas O. Olwal, Michael A. van Wyk and Barend J. van Wyk

Abstract—In this paper we present a soft timing phase estimation (STPE) method for wireless mobile receivers operating in low signal to noise ratios (SNRs). Discrete Polyphase Matched (DPM) filters, a Log-maximum a posterior probability (MAP) and/or a Soft-output Viterbi algorithm (SOVA) are combined to derive a new timing recovery (TR) scheme. We apply this scheme to wireless cellular communication system model that comprises of a raised cosine filter (RCF), a bit-interleaved turbo-coded multi-level modulation (BITMM) scheme and the channel is assumed to be memory-less. Furthermore, no clock signals are transmitted to the receiver contrary to the classical data aided (DA) models. This new model ensures that both the bandwidth and power of the communication system is conserved. However, the computational complexity of ideal turbo synchronization is increased by 50%. Several simulation tests on bit error rate (BER) and block error rate (BLER) versus low SNR reveal that the proposed iterative soft timing recovery (ISTR) scheme outperforms the conventional schemes.

Keywords—discrete polyphase matched filters, maximum likelihood estimators, soft timing phase estimation, wireless mobile systems.

I. INTRODUCTION

IN the recent past, most wireless mobile communication systems have over-relied on classical forward error correction (FEC) codes to either save bandwidth or reduce power requirements [1]. However, classical FEC coding schemes have limited coding gain. In particular, wireless cellular mobile receivers in a number of recent publications employ data-aided (DA) synchronizers [2]. Such synchronizers are based on the Viterbi algorithm (VA) for optimum signal detection to achieve accuracy, reliability and fast speed convergence. However, DA timing phase recovery is the bandwidth and power inefficient since additional bandwidth and power are needed to transmit clock signals to the receiver. Several receiver functions such as the signal detection, equalization, demodulation and timing recovery, are now possible with a combined turbo decoding algorithm [3]-[5].

T. Olwal is with the Council for Scientific and Industrial Research (CSIR), Pretoria, South Africa (phone: +27 12 841 2085; fax: +27 12 841 4829; e-mail: thomas.olwal@gmail.com).

M. A. van Wyk is with the University of Witwatersrand, Jhb, South Africa (e-mail: mavanwyk@gmail.com).

B. J. van Wyk is with the Engineering Faculty, Tshwane University of Technology, Pretoria, South Africa (e-mail: vanwykb@@gmail.com).

Most classical timing phase estimation schemes can be separated from the decoding process with little penalty: This is because the timing recovery uses instantaneous decision device to provide tentative decisions that are adequately reliable. The reliable decisions are used to estimate the timing phase error [6]. Classical timing recovery methods also assume that the neighbouring symbols are mutually independent at high SNR and the associated theoretical framework is normally based on the least mean square (LMS) and traditional phase-locked loops (PLL) [7]. Such a framework is susceptible to local minima and often presents additional block processing complexities which fail in low SNR conditions.

The results in [8], [9] have shown that classical soft-input/soft-output (SISO) iterative detection/decoding algorithms (IDDA) embed the timing parameter estimation in the decoding process. For instance in [9], a combined iterative decoding, equalization and timing error estimation is performed with the modified forward and backward recursions in the SISO decoders using a per-survivor processing algorithm [15]. Such methods are reliable but increase the receiver's design complexity with a vast memory requirement. In order to reduce the complexity involved in designing the decoder structure, the soft information generated by the turbo receiver are exploited to derive reliable signals on timing error estimation. This process is known as the turbo principle synchronization technique [16]. Though recent research attention has focused on turbo synchronization methods [4], [5], achieving a fast converging timing recovery process has been under investigated. Unlike in [4], [5] we derive soft timing phase offsets from a discrete polyphase matched filtering receiver [16] producing asynchronous samples. Furthermore, modelling a timing phase offset as a vector quantity embedded in a time division multiplexing access (TDMA) block or frame in cellular networks not only achieves a realistic model representation but also motivates the need for designing a bandwidth and power efficient transmitter system. The BER and BLER performances can easily be investigated for the derived communication system and time recovery scheme.

The objective of this paper is to develop a soft and fast timing recovery method for wireless cellular mobile receivers. This goal is achieved by combining discrete polyphase matched (DPM) filtering with asynchronous samples, an

iterative soft demapper- turbo decoder (ISDTD) and a modified Newton Raphson (MNR) method.

This paper is organized as follows. Section I provided a broad overview of the problem. In section II, the baseband turbo system model is presented. In section III, a soft timing recovery framework is proposed. Simulation tests and results are presented in sections IV. A brief computational complexity analysis and conclusions are presented in sections V and VI, respectively.

II. MOBILE COMMUNICATION SYSTEM MODEL

A. The Channel Model

Let us consider a baseband equivalent of a cellular transmitter model proposed by Dejonghe *et al.* [25] and Olwal *et al.* [24] in which the raised cosine pulse shaping filter (RCPSF) [7] output is given by

$$s(t) = \sum_{k=0}^K a_k g(t - kT), \quad (1)$$

where $g(t)$ is the filter impulse response in time domain, a_k is the k th complex symbol and T is the symbol period $0 \leq k \leq K$, observed over a large interval.

The wireless terrestrial radio propagation of mobile traffic suffers from delays and attenuations due to multipath fading. The multipath fading is modelled by a linear time-variant filter characterized by the complex-valued low-pass equivalent channel impulse response (CIR)

$$h_c(t) = \sum_{n=1}^N \alpha_n(t) e^{j\phi_n(t)} \delta(t - \tau_n(t)). \quad (2)$$

Here, N is the number of propagation paths modelled as filter taps, $\alpha_n(t)$ is the amplitude, $\phi_n(t)$ is the phase, and $\tau_n(t)$ is the timing phase shift, respectively of the mobile signal passing through an n th radio channel path. If we hypothesize that in TDMA $\tau_n(t)$ is separated from $\tau_{(n+1)}(t)$ at symbol rate then the following statistical definitions can be assumed to be $T_d \leq T \leq T_c$, where T_d the delay spread which must satisfy is

$$\sup_{n, n+1, t} |\tau_n(t) - \tau_{(n+1)}(t)| \leq T_d \quad (3)$$

and T_c is the coherence time.

This delay spread described by (3) measures in part the radio channel scattering effects hence a contribution to multipath fading. The amplitude of the multipath fading is modelled as Rayleigh distribution with no line-of-sight (LOS) path.

On the other hand f_c must satisfy

$$\sup_{s, n, t; |s-t|} f_c [\tau_n(t) - \tau_n(s)] \ll 1, \quad (4)$$

where f_c is the carrier frequency of the pass-band signal, $\tau_n(t)$ and $\tau_n(s)$ are the timing offsets of the n th path

observed at different times, t and s respectively. The coherence time is thus, the period over which the pass-band cellular signal essentially remains time invariant. These statistical definitions presented in (3) and (4) allow the continuously time varying signal to be assumed as an ergodic and piecewise-constant stochastic process. After the above analysis, the transmitted signal in (1) is convolved with the CIR in (2) and passed through an additive white Gaussian noise (AWGN) for atmospherically generated interferences.

B. The Receiver System Model

In general, the received signal vector \mathbf{r} becomes,

$$r(t) = \sum_{n=1}^N \alpha_n(t) s(t - \tau_n(t)) e^{j\phi_n(t)} + n(t). \quad (5)$$

Here, $n(t)$ is the time-variant additive white Gaussian noise with independent and identical distribution and variance is $N_0 / 2$. Applying (1) to (5) yields,

$$r(t) = \sum_{n=1}^N \alpha_n(t) e^{j\phi_n(t)} \left\{ \sum_{k=0}^{K-1} [a_k g(t - kT - \tau_n(t))] \right\} + n(t). \quad (6)$$

In estimating the timing offset, the received signal is passed through a channel diversity combiner that equalises multipath delay line channels to match the K transmitted symbols each with a time delay $\tau_k(t)$. Moreover, $\tau_n(t)$ was assumed separated from $\tau_{n+1}(t)$ at a symbol rate, $1/T$. The (6) can be re-written as,

$$r(t) = \sum_{n=1}^N A_n(t) \left\{ \sum_{k=0}^{K-1} a_k g(t - kT - \tau_k(t)) \right\} + n(t), \quad (7)$$

where $A_n(t) = \alpha_n(t) e^{j\phi_n(t)}$, is a nuisance parameter and is independent on the time delay $\tau_k(t)$. The notation $\{\tau_k(t)\}$ is a set of time varying k th symbol timing offset parameter to be estimated over a K set in a TDMA frame. In order to collect sufficient statistics for decoding module, the received signal is low-pass filtered by anti-aliasing filter then sampled asynchronously at a rate of $1/T_s$, where $T_s < T/(1+\alpha)$. The asynchronous samples satisfy the Nyquist sampling theorem $f_s \geq 2/T$. (where $f_s = 1/T_s$).

Neglecting the nuisance parameter in (7) and taking L samples over each symbol, the total samples of the observation vector \mathbf{r} will be KL . The vector \mathbf{r} can be re-defined as,

$$\begin{aligned} r_l &\cong r(lT_s) \\ &= \sum_{k=0}^{LK-1} a_k g(lT_s - kT - \tau_k(lT_s)) + n(lT_s). \end{aligned} \quad (8)$$

C. Discrete Polyphase Matched (DPM) filtering

In order to achieve the required timing resolution of $M \times L$ samples per symbol from timing phase-corrected complex baseband signal given in (8), an up-sampling of $r(lT_s)$ by a factor of M to obtain $r(lT_s/M)$ must be performed. The resulting signal is filtered via a DPM root raised cosine filter whose output yields

$$y(lT_s/M) = \sum_{k=0}^{MLK-1} r((l-k)T_s/M)g(kT_s/M). \quad (9)$$

The matched filter output is down sampled to produce L samples per symbol where one of the samples is as close to $y(lT_s + \tau_k)$ as the resolution allows. Because M up sampling rate introduces zero padding between every sample in all L samples per symbol, the polyphase decomposition of $r(lT_s/M)$ yields only M th nonzero values of the FIR filter output,

$$r(lT_s/M) = \begin{cases} r(lT_s), & l = 0, M, 2M, \dots \\ 0, & \text{otherwise} \end{cases} \quad (10)$$

At initial timing instant, these nonzero values in (10) coincide with the filter coefficients $g(0), g(MT_s), g(2MT_s) \dots$ and the DPM filter output may be expressed as

$$y(lT_s) = \sum_{i=0}^{LK-1} r((l-i)T_s)g(iT_s). \quad (11)$$

At the next timing instant, the nonzero values in (11) coincide with the filter coefficients $g(1), g(MT_s+1), g(2MT_s+1)$, and the DPM filter output is expressed as

$$y((l-1/M)T_s) = \sum_{i=0}^{LK-1} r((l-i)T_s)g((i+1/M)T_s). \quad (12)$$

At the m th timing instant, the nonzero values in (12) coincide with the coefficients $g(m), g(MT_s+m), g(2MT_s+m), \dots$ and the DPM filter output is,

$$y((l-m/M)T_s) = \sum_{i=0}^{LK-1} r((l-i)T_s)g((i+m/M)T_s). \quad (13)$$

From the (11) through (13), M filter-banks have simultaneously input data samples $r(lT_s)$ and the desired timing phase shift of the matched filter output is selected by connecting the matched filter output to appropriate filter in the filter-bank. However, the timing phase shift is unknown exactly and soft decision iterative turbo receiver is employed to generate reliable estimates [5]. In this sequel, the maximum likelihood estimation (MLE) of the desired phase shift from SISO exchanges will be derived.

III. SOFT TIMING RECOVERY

A. Estimating soft timing information

The problem addressed in this section is the estimation of the time delay vector in a TDMA frame, $\boldsymbol{\tau} = [\tau_0, \tau_1, \dots, \tau_{K-1}]^T$ subject to a trial $\tilde{\boldsymbol{\tau}} = [\tilde{\tau}_0, \tilde{\tau}_1, \dots, \tilde{\tau}_{K-1}]^T$ generated by the DPM filter. This estimate may be seen as the solution of the maximization problem [24]

$$\hat{\boldsymbol{\tau}} = \underset{\tilde{\boldsymbol{\tau}}}{\operatorname{argmax}} \Lambda(\tilde{\boldsymbol{\tau}}). \quad (14)$$

Here,

$$\Lambda(\tilde{\boldsymbol{\tau}}) = \ln p(\mathbf{y} | \mathbf{a}; \tilde{\boldsymbol{\tau}}) \quad (15)$$

and

$$p(\mathbf{y} | \mathbf{a}; \tilde{\boldsymbol{\tau}}) = \int P(\mathbf{a}) p(\mathbf{y} | \mathbf{a}; \tilde{\boldsymbol{\tau}}) d\mathbf{a}, \quad (16)$$

where $P(\mathbf{a})$ is a prior probability mass function (PMF) and is assumed unknown to the receiver. The PMF will be derived from posterior information. Variables \mathbf{a} and $\tilde{\boldsymbol{\tau}}$ are assumed mutually independent vectors to each other but dependent on a complex vector \mathbf{y} . Equation (16) is referred to as the joint likelihood function (JLF) and can be used to estimate both the vector $\boldsymbol{\tau}$ and a nuisance vector \mathbf{a} . From (16), the JLF $p(\mathbf{y} | \mathbf{a}; \tilde{\boldsymbol{\tau}})$ is given by

$$p(\mathbf{y} | \mathbf{a}; \tilde{\boldsymbol{\tau}}) = \prod_{k=0}^{K-1} \Phi(a_k; \tilde{z}_k(\tilde{\tau}_k)), \quad (17)$$

where from [26] and after the DPM filtering we have, $\Phi(a_k; \tilde{z}_k(\tilde{\tau}_k)) = \exp\{\Re(a_k^* \tilde{z}_k(\tilde{\tau}_k) - |a_k|^2)\}$. Here, $\tilde{z}_k(\tilde{\tau}_k)$ can be defined by an output of the DPM filter as,

$$\tilde{z}_k(\tilde{\tau}_k) \approx y(lT_s + \tilde{\tau}_k). \quad (18)$$

Applying (18) into (17) we have,

$$p(\mathbf{y} | \mathbf{a}; \tilde{\boldsymbol{\tau}}) = \prod_{k=0}^{K-1} \exp\{\Re(a_k^* y(lT_s + \tilde{\tau}_k) - |a_k|^2)\}. \quad (19)$$

Applying \log to (19) and neglecting terms independent on $\tilde{\tau}_k$ we have,

$$\ln p(\mathbf{y} | \mathbf{a}; \tilde{\boldsymbol{\tau}}) \cong \Re\left\{\sum_{k=0}^{K-1} a_k^* y(kT + \tilde{\tau}_k)\right\}. \quad (20)$$

In order to solve (14), we take the derivative of (20) with respect to $\tilde{\boldsymbol{\tau}}$ which we equate to a zero vector, namely

$$\frac{\partial}{\partial \tilde{\boldsymbol{\tau}}} \ln p(\mathbf{y} | \mathbf{a}; \tilde{\boldsymbol{\tau}}) = \mathbf{0}. \quad (21)$$

In this sequel, a solution related to the work in [12], [22], [24] is proposed. Here, a set of values for

$\hat{\boldsymbol{\tau}} = \{\hat{\tau}^1 \dots \hat{\tau}^1 \dots \hat{\tau}^n\}$ is a possible solution, where n is the iteration number satisfying final limit property that as $n \rightarrow \infty$ the sequence of timing estimate converges to a desired

solution. All independent parameters of $\tilde{\tau}$ are ignored. The posterior outputs in (21) of iterative receiver can then be equivalently approximated with priors as follows:

$$\begin{aligned} &\cong \sum_{k=0}^{K-1} \left[\Re \left\{ P(a_k) a_k^* \frac{\partial}{\partial \tilde{\tau}_k} y(kT + \tilde{\tau}_k) \right\} \right]_{\tilde{\tau}=\hat{\tau}} = \mathbf{0}, \\ &= \sum_{k=0}^{K-1} \Re \left\{ \left[\sum_{\mathbf{a} \in \mathbf{B}} a_k^* (x_k^1, x_k^2, \dots, x_k^Q) P(a_k(x_k^1, x_k^2, \dots, x_k^Q)) \right] \dot{y}(kT + \hat{\tau}_k) \right\} = \mathbf{0}. \end{aligned} \quad (22)$$

Here, we let

$\eta_k^* = \sum_{\mathbf{a} \in \mathbf{B}} a_k^* (x_k^1, x_k^2, \dots, x_k^Q) P(a_k(x_k^1, x_k^2, \dots, x_k^Q))$, and it is defined as a prior mean information complex conjugate variable describing the transmitted symbol, a_k . The transmitted symbol in (22) is composed of the Q coded bits in a multilevel symbol modulation scheme (MSMS) [22].

According to [19], the soft information demapper computes posteriori probabilities from bit priori probabilities in low SNR environments. This is performed as follows,

$$\begin{aligned} P(x_k^1, x_k^2, \dots, x_k^Q) &\approx P(x_k^1) P(x_k^2) \dots P(x_k^Q), \\ &\triangleq \prod_q P(x_k^q). \end{aligned} \quad (23)$$

The soft demapper also computes soft information defined by the log-likelihood ratio (LLR), $\lambda^{12}(x_k^q | \mathbf{y}; p)$, on each a posteriori probability in order to achieve a wider dynamic range of decision levels as follows:

$$\lambda^{12}(x_k^q | \mathbf{y}; p) = \lambda^{12}(x_k^q | \mathbf{y}; e) + \lambda^{12}(x_k^q; i). \quad (24)$$

Here, $\lambda^{12}(x_k^q; i)$, is referred to as intrinsic information computed from the demapper to the decoder and the extrinsic information, $\lambda^{12}(x_k^q, \tilde{\tau}_k | \mathbf{y}; e)$, is defined as,

$$\lambda^{12}(x_k^q, \tilde{\tau}_k | \mathbf{y}; e) = \log \frac{\sum_{\forall \mathbf{x}: x_k^q=0} P(\mathbf{y} | \tilde{\tau}, \mathbf{x} \in \mathbf{B}) \prod_{i=1: i \neq k}^{2N} P(x_{\forall k}^i)}{\sum_{\forall \mathbf{x}: x_k^q=1} P(\mathbf{y} | \tilde{\tau}, \mathbf{x} \in \mathbf{B}) \prod_{i=1: i \neq k}^{2N} P(x_{\forall k}^i)}. \quad (25)$$

As shown in [3], the log-maximum a posteriori (Log-MAP) decoding algorithm of (25) becomes,

$$\lambda^{21}(b_k^q, \tilde{\tau}_k; p) = \log \frac{P\{b_k^q = 0 | \lambda^{21}(\mathbf{c}; i), \lambda^{21}(\hat{\mathbf{b}}; i), decode\}}{P\{b_k^q = 1 | \lambda^{21}(\mathbf{c}; i), \lambda^{21}(\hat{\mathbf{b}}; i), decode\}} \forall k. \quad (26)$$

Here, $\lambda^{21}(b_k^q, \tilde{\tau}_k; p)$, is the Log-MAP information computed on bits from the decoder to demapper module. On the other

hand, the Viterbi algorithm [20] computes the SISO from (25), as follows

$$\lambda^{21}(a_k, \tilde{\tau}_k; p) = \frac{1}{\alpha} \log \frac{1 + e^{(\alpha \lambda^{21}(a_k; i) + \Delta)}}{e^{(\Delta)} + e^{(\alpha \lambda^{21}(a_k; i))}}, \quad (27)$$

where, $\lambda^{21}(a_k, \tilde{\tau}_k; p)$, is the soft output Viterbi algorithm (SOVA) posterior information computed on symbols output from the decoder to demapper module. The notations, $\alpha = 4d_{free} E_s / N_0$ and Δ are the two path metric differences in the trellis structure presented in [20]. Exploiting the Log-MAP and SOVA based SISO computations in (26) and (27), the posterior means (PM) in (22) yields,

$$\eta_k = \sum_{\mathcal{G}_m \in \mathbf{B}} \mathcal{G}_m P(a_k = \mathcal{G}_m | \mathbf{y}, \tilde{\tau}_k), \quad (28)$$

where \mathcal{G}_m is a real scalar symbol value from B-possible modulation constellation signal set. From [19] together with (23) through (27) detailed derivation yield posterior probabilities (APPs):

$$P(a_k = \mathcal{G}_m, \tilde{\tau}_k | y_k) = \frac{\exp(-\mathcal{G}_m \lambda^{21}(a_k = \mathcal{G}_m, \tilde{\tau}_k | y_k))}{1 + \exp(-\lambda^{21}(a_k = \mathcal{G}_m, \tilde{\tau}_k | y_k))}. \quad (29)$$

The a priori mean information in (22) is now approximated as a posteriori mean information in (28). Equations (26) and (27) present the log-MAP and SOVA based timing recovery methods, respectively. The log-MAP and SOVA based timing recovery equations are substituted in (28) for soft mean information. The soft mean information generates the soft timing phase signals. This is achieved through several iterations by the soft demapper-decoder system. The reliable soft timing phase signals are attained after the system has converged. Soft timing phases estimated in (28) update the DPM filter.

B. Timing Estimates Update

We begin the iteration by assuming that the previous, $(i-1)$ th timing offset estimate is zero. The estimated timing offset finally updates the early and late samples of the DPM filter outputs and an optimal synchronization is attained when the early and late samples become equal [22]-[25]. The new timing estimate will be based on the DPM filter output $y(s)|_{s=kT+\hat{\tau}^{i-1}}$ as shown in Fig. 1 and the mean of posterior probabilities $\eta_k^{(i-1)}$ from the previous iteration according to (29) and [24].

IV. SIMULATION TEST AND RESULTS

To verify the performance of our turbo aided timing recovery scheme, we simulated a baseband communication

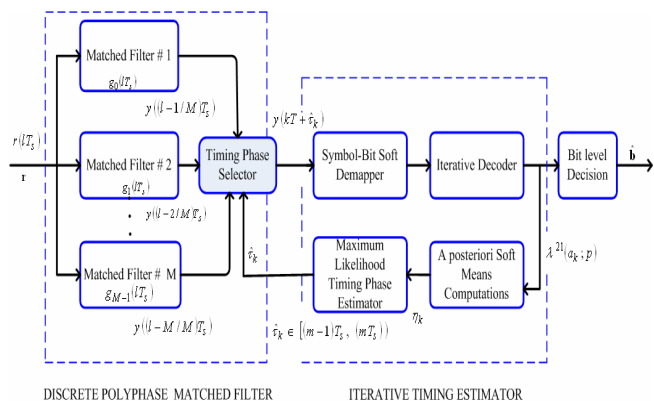


Fig. 1: The iterative timing recovery receiver structure

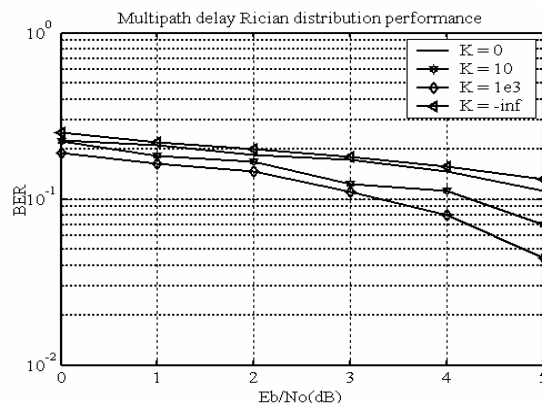


Fig. 2: Wireless cellular radio channel performance

Open Science Index, Electronics and Communication Engineering Vol:3, No:4, 2009 publications.waset.org/3493.pdf

system transmitting an 8-constellation alphabet for phase shift keying (8-PSK) symbols in MATLAB. We considered a convolutional turbo code generator polynomial $(23, 35)_8$ with punctured net rate of a $1/2$. The interleaver length consists of 456 bits. An RCPSF with roll-off of 0.35 and 31 filter taps was employed. 1000 blocks were transmitted over a Rician distributed fading channel with an AWGN. The received signal was passed through an anti-aliasing filter and then sampled at an incommensurate rate but higher than the baud rate or the symbol rate. A DPM filtering structure was embedded at the input of the SDTD to help with fast iterative soft timing phase estimation (ISTPE). In order to investigate for bit error rate (BER) and radio block error rate (BLER) performance, a Monte Carlo simulation methodology [21] was performed for an evolved GSM communication system (EDGE).

Results in Fig. 2 reveal a typical radio channel BER performance for a wireless mobile system. For simplicity in radio channel modelling, multipath flat fading is described by a Rician K -factor denoted by $K = \beta^2 / 2\sigma_0^2$. Here, β and σ_0^2 are the amplitude of the specular path component (dominant line of sight) and variance of Gaussian random channel samples with zero-means, respectively. For instance, a zero value of K , means that there is no line-of-sight (LOS) between the transmitter and the receiver. In such scenarios, a Rician channel distribution is best modelled by a Rayleigh channel distribution. The Rayleigh channel distribution reveals severe channel conditions. The BER performance of synchronizers in Figure 3 is worst when $K = -\infty$. It is necessary that wireless mobile receivers operating at a low SNR, require turbo codes to generate reliable soft timing estimates after many turbo iterations. This ensures a guaranteed QoS provisioning to end users at the expense of latency. In voice based receivers, latency is highly undesirable. Thus the generation of soft timing estimates is a trade off between number of turbo iterations and perfect synchronization.

The bit error rate (BER) performance of an iterative soft timing recovery (ISTR) based on the logarithmic maximum likelihood a posteriori (Log-MAP) information is depicted in Fig. 3. The soft information based on a combined ML and iterative turbo timing recovery (ITTR) method outperforms conventional methods. The results in Fig. 3 reveal desirable BER performances: steady waterfall and minimum error floor region within a short span of a SNR at low measurements, i.e. 1-2.5dB. The proposed method yields low BER compared to a data-aided Viterbi detection (DAVD) based synchronizer and a classical early-late gate (ELG) synchronizer. This is explained by the fact that in low SNR scenarios, data aided (DATR) and early-late gate (ELGTR) methods assume that neighbouring symbols of the received signal are statistically independent and thus the received signal is deterministic a priori. However, the assumption fails in severe channel distortions. The receiver must therefore resort to blind timing recovery (BTR) methods. In the proposed method, the unknown a priori bit probabilities are approximated by posteriori computations.

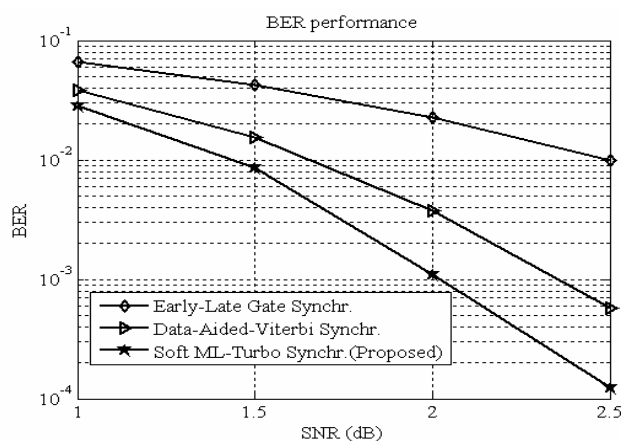


Fig. 3: Log-MAP based soft timing recovery method for BER

In Fig. 4 the block error rate (BLER) performance of an ISTR based on the Log-MAP information is shown. The proposed method outperforms conventional methods. In the log-MAP based timing recovery (TR) scheme, the BER and

BLER perform well at low SNR, which is highly desirable for wireless cellular mobile systems. In recent publications DATRs are known to be more reliable than the classical decision-directed timing recovery (DDTR), but the BER and BLER performance indicated by Fig. 3 and 4 respectively, show that the proposed TR scheme yields a better performance. This is because of stochastic channel conditions and low SNR environments that make it difficult for the receiver to extract correct clock signals from the received sequence. Unlike classical DDTR methods that give decisions from the limited dynamic probability range i.e. probability value range from 0 to 1, the proposed method has a larger dynamic range for making decisions i.e. soft information are represented with probability ratios which range from 0 to infinity.

The results in Fig. 5 show the soft output Viterbi algorithm (SOVA) BER performance compared to conventional methods. Like in log-MAP based synchronizers, the BER performance indicates desirable start-up, waterfall and error regions. The results indicate that the proposed method outperforms the conventional methods and the explanations motivating this observation are similar to the discussions for Fig. 3. However, the DATR method performed closer to the proposed SOVA method. This can be explained by the fact that SOVA based turbo structures yield soft timing signals (STS) from signal sequences similar to simple Viterbi based detectors. However, due to turbo codes, the proposed TR in SOVA performs well in low SNR channels compared to the classical FEC codes in conventional methods.

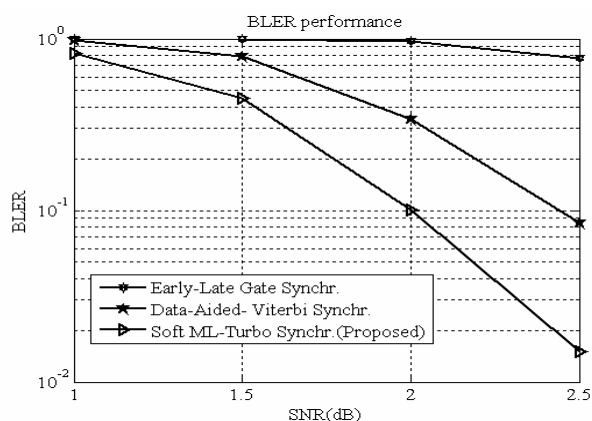


Fig. 4: Log-MAP based soft timing recovery method for BLER

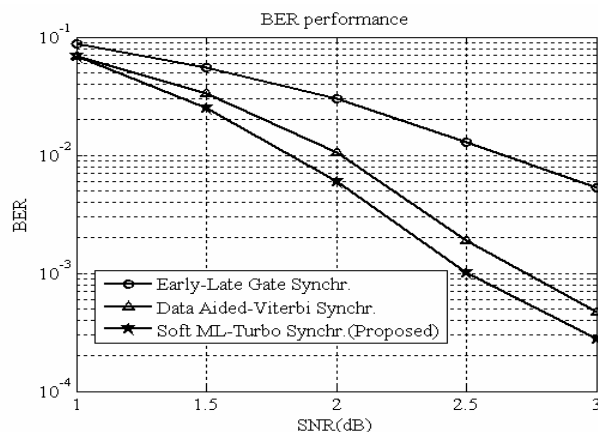


Fig. 5: SOVA based soft timing recovery method for BER

The SOVA based timing recovery BLER performance compared to conventional methods are depicted in Fig. 6. The proposed method provides lower BLER performance than conventional methods. The ELGTR yields the worst BLER performance in low SNR. This is due to the fact that the associated matched filter aiding the ELGTR schemes is sub-optimal when neighbouring symbols are statistically dependent in noisy channels. In general, the BER and BLER of the proposed TR method indicate good error floor, waterfall and start-up regions as expected. However, overall simulation results indicate that SOVA based timing recovery methods yield a degraded BER and BLER performance in low SNR compared to the log-MAP methods. The reason behind this can be explained by the fact that log-MAP timing recovery methods are computed at individual bit level decision with high and required resolution to correct channel errors while the SOVA based TR method operates at symbol level with low decision resolution. Moreover, bit sequences were interleaved at the transmitter end before being mapped in a spectrally efficient digital modulator. This bit level interleaving corrects error bursts more effectively than performing the interleaving at symbol level. Since turbo receivers employ a bit by bit demapper and de-interleaver, the presence of channel error bursts can easily be corrected. This leads to low BER and BLER performance and consequently improved QoS provisioning to the terminal mobile users. However, log-MAP based soft timing recovery methods yield more reliable STS at the expense of receiver's computational and structural complexities. The complexities constrain the mobile system's memory and battery power requirements. Such requirements are undesirable for mobile system operators. Thus, SOVA based STR methods become an alternative method to provide QoS demands by both mobile operators and end users. However due to the presence of multiple nuisance parameters characterising the log-MAP and SOVA based soft timing estimators, the timing error variance must be investigated.

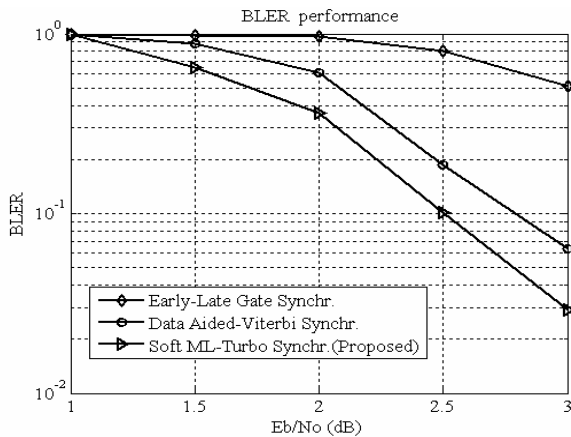


Fig. 6: SOVA based soft timing recovery method for BLER

V. COMPUTATIONAL COMPLEXITY OF THE RECEIVER

In this sequel, a brief computational analysis is delimited to the evaluation of the required number of floating point operations, namely additions and multiplications [5]. Comparisons and table lookups form the basis of future work. The computational load of a STPE receiver comprises the DPM filter, iterative joint demapping-decoding (IJDD) and an ISTPE (c.f. Fig. 1). An attempt to reduce the overall computational complexity and latency is ensured by allowing only one IJDD and ISTPE operation at each of the system's iteration. For the sake of simplicity, let N be the TDMA frame length, s the number of states of the rate $\frac{1}{2}$ RSC component decoder, K the number of transmitted 8-PSK symbols and n the number of the receiver system's iterations. We can denote computational complexity (CC) by $\Omega_{i \in \mathbb{R}}$.

The raised cosine pulse shaping filter (RCPSF) implements the DPM filtering with impulse response that occupies 31 taps with sampling frequency, $f_s = 1.35/T$ and an 8-PSK modulation scheme is used. For K symbols the computational complexity (CC) $\Omega_0 \cong 126.K$.

Each SISO evaluates APPs for the systematic bits [5]. In each receiver system's iteration, two SISO decoders are employed, which compute the Max-Log-MAP [27]. The CC becomes $\Omega_1 \cong 24s.N.n$ for Log-MAP and $\Omega_1 \cong 24s.K.n$ for SOVA operations respectively. In the ISTPE, the APPs for the parity bits are required as well. This must be computed by the two SISO decoders. The CC becomes $\Omega_2 \cong 12s.N.n$ for the Log-MAP and $\Omega_2 \cong 12s.K.n$ for the SOVA operations respectively.

The initial metrics required by the IJDD modules are produced by the DPM after phase compensation. For an 8-PSK modulation scheme, there are three bits in every symbol [19]. The additional CC in computing these metrics will become $\Omega_3 \cong 3K.n$. In Equations (36) and (37), the posterior means (PM) and a posterior probability (APP) respectively, were computed at each an IJDD iteration with a relevant computational complexity of the operation that amount to $\Omega_4 \cong 6K.n$. The final task, the ITPE receiver must perform is the updating of the timing phase estimates. Other than ELG

comparisons involved the relevant CC with MNR method becomes $\Omega_5 \cong 3K.n$.

The overall computational complexity of the proposed ITPE receiver amounts to

$$\Omega_{ITPE} = \sum_{i=0}^5 \Omega_i \cong 126K + 36s.N.n + 12K.n \quad (30a)$$

$$\cong 126K + 36s.K.n + 12K.n \quad (30b)$$

The equation (30a) reveals a CC in the number of bits other than symbol level complexity revealed by (30b). In the CC comparisons with the conventional timing recovery (CTR) schemes, the CC employs the following formula[5]:

$$\Delta\Omega = \frac{\Omega_{ITPE} - \Omega_{CTR}}{\Omega_{CTR}} . 100. \quad (31)$$

The data-aided Viterbi synchroniser's CC,

$\Omega_{CTR(DA)} \cong 126K + 36s.N.n$ whereby the Viterbi Algorithm (VA) is the main computational load. The additional computational load introduced by the proposed ITPE is computed according to (31), is approximately

$$\Delta\Omega_{CTR(DA)} \approx 80\%. \quad (32)$$

Similarly, the early-late gate (ELG) synchroniser's CC is $\Omega_{CTR(ELG)} \cong 126K + 12K.n$. Here, there is no SISO computation involved. The additional computational complexity is approximately

$$\Delta\Omega_{CTR(ELG)} \approx 72\%. \quad (33)$$

Finally, the Ideal turbo synchronization [17] has the computational complexity denoted by

$\Omega_{CTR(IDEAL)} \cong 126K + 24s.N.n + 3K.n$. The additional computational complexity is given by

$$\Delta\Omega_{CTR(IDEAL)} \approx 50\%. \quad (34)$$

The numerical approximations of the computational complexities indicate that the proposed ITPE receiver demonstrate high level of complexity compared to the CTR schemes. The extra computational load is mainly due to the evaluation of the posterior probabilities (APPs) of parity bits. To reduce this phenomenon, one may use other channel coding schemes such as serially-concatenated convolutional codes (SCCC) and low-density parity check (LDPC) available in literature [7].

VI. CONCLUSION

The bit error rate (BER) simulation test in Fig. 4 indicates that the proposed soft timing phase estimation method outperforms both ELG and DAVTR schemes. This is because in low signal to noise ratio (below 2.5dB) the transmitted symbols are statistically independent hence the classical phase locked loops for synchronisation fail to yield low BER

performance. The exploitation of turbo code properties is desirable in such situations. Similar observation was noted in Figure 6 when a test for BLER was performed. However, the overall performance degraded for the BLER test. This is because the proposed combined turbo and DPM filter performs Log-MAP based TR algorithm at bit level. Moreover at block level there is high possibility of channel error burst propagation.

In Fig. 5 and 6, the simulation tests showed that the proposed ISTPE method outperforms the classical TR schemes at low signal to noise ratios (below 3dB). However, since the SOVA based timing recovery method are performed at symbol level rather than bit level, the observed BER and BLER results were slightly poorer than Log-MAP based TR methods.

However, the proposed method is computationally complex compared to the DAVTR schemes. The complexity can be traded-off for efficient power and bandwidth required by most mobile receiver systems.

ACKNOWLEDGMENT

The authors would like to acknowledge CSIR and Tshwane University of Technology for their support.

REFERENCES

- [1] A. Shanmugam and A. R. Abdul Rajak, "Optimal design of forward error correcting codes for wireless communication", *www.academicjournal.com*, vol. 14, 2005.
- [2] CISCO, "Cisco mobile exchange solution guide: Overview of GSM, GPRS, and UMTS", *www.cisco.com*, 2002.
- [3] M. Sellathurai and S. Haykin, "Turbo-Blast for wireless communications: theory and experiments," *IEEE Trans. Sig. Proc.*, vol. 50, no. 10, pp. 2538-2546, 2002
- [4] C. Herzet, V. Ramon, L. Vandendorpe, "Iterative soft-decision directed timing estimation for turbo receivers," *IEEE 9th Symposium on Commun., and Vehicular Technology*, pp. 97-101, 2003
- [5] N. Noels, V. Lottici, A. Dejonghe, H. Steendam, M. Moeneclaey, M. Luise, L. Vandendorpe, "A theoretical framework for soft-information-based synchronization in iterative(turbo) receivers," *EURASIP J. Wireless Commun., and Network.*, vol. 2, pp. 177-129, 2005.
- [6] K. H. Mueller and M. Muller, "Timing recovery in digital synchronous data receivers," *IEEE Trans. Commun.*, vol. Com-24, pp. 516-532, 1976.
- [7] J. G. Proakis and M. Salehi, *Communication systems engineering*. New Jersey: Prentice Hall, 2002.
- [8] J. R. Barry, A. Kavcic, S. W. McLaughlin, A. Nayak, and W. Zeng, "Iterative timing recovery," *IEEE Signal Processing Mag.*, vol. 2, pp. 89-102, 2004.
- [9] P. Kovintavewat, J. R. Barry, M. F. Erden, and E. M. Kurtas, "Robustness of per-survivor iterative timing recovery in perpendicular recording channels," *IEEE Trans. Magnetics*, vol. 10, pp. 807-808, 2005.
- [10] B. Mielczarek, *Turbo codes and channel estimation in wireless systems*, PhD Thesis, Signals and Systems, Chalmers University of Technology, Goteborg, 2002.
- [11] J. M. Walsh, C. R. Johnson, and P. A. Regalia, "Joint synchronization and decoding exploiting the turbo principle," in *Proc. Conf. Inform. Sciences and Systems*, 2004
- [12] D. Tabak and B. C. Kuo, *Optimal control by mathematical programming*. New Jersey: Prentice Hall, 1971.
- [13] H. Meyr, M. Moeneclaey, and S. Fechtel, *Digital communication receivers: Synchronization, channel estimation, and signal processing*. New York: John Wiley and sons, 1998.
- [14] A. Nayak, J. Barry and S. McLaughlin, "Joint Timing Recovery and Turbo Equalization for Coded Partial Response Channels," *IEEE Trans. Magnetics*, vol. 38, no.5, pp. 2295-2297, Sept 2002.
- [15] F. J. Harris and M. Rice, "Multirate digital filters for symbol timing synchronization in software defined radios," *IEEE journal on selected areas in commun.*, vol. 19, no. 12, pp. 2346-2357, 2001.
- [16] F. J. Harris, *Multirate signal processing for communication systems*. New Jersey: Prentice Hall, 2004.
- [17] N. Noels, C. Herzet, A. Dejonghe, et al., "Turbo synchronization: an EM interpretation," In *Proc. IEEE international Conference on Communications (ICC '03)*, Anchorage, Alaska, USA, May 2003.
- [18] N. Noels, H. Wymeersch, H. Steendam and M. Moeneclaey, "The true Cramer-Rao bound for timing recovery from a bandlimited linearly modulated waveform with unknown carrier phase and frequency," *IEEE Trans. Commun.*, vol. 52, no. 3, pp. 473-483, March 2004.
- [19] R. Koetter, A.C. Singer and M. Tuchler, "Turbo equalization," *IEEE Signal Processing Magazine*, vol. 21, no. 1, pp. 67-80, January 2004.
- [20] J. Hagenauer and P. Hoher, "A Viterbi algorithm with soft-decision outputs and its applications," *IEEE Trans. Commun.*, vol. 47, pp. 1680-1686, 1989.
- [21] N. Metropolis and S. Ulam, "The Monte Carlo method," *American Statistic Association Journal*, vol. 44, pp. 335-341, 1949.
- [22] T. O. Olwal, M. A. van Wyk, D. Chatelain, M. Odhiambo and B. J. van Wyk, "Low variance timing recovery in turbo receivers," In *Proc. IEEE 13th International Conference on Telecommunication (ICT '06)*, Funchal, Portugal, May 2006.
- [23] T. O. Olwal, M. A. van Wyk, D. Chatelain, M. Odhiambo and B.J. van Wyk, "Cramer-Rao bound on timing recovery for GSM receivers," In *Proc. IEEE ICTe Africa2006*, Nairobi, Kenya, May 2006.
- [24] T. O. Olwal, M. A. van Wyk, B. J. van Wyk, M. Odhiambo and D. Chatelain, "Improved timing recovery in wireless mobile receivers" *African Journal of Science and Technology (AJST)*, vol. 8, no. 1, pp. 71-86, 2007.
- [25] A. Dejonghe, X. Jaspar, X. Wautelet and L. Vandendorpe, "Assessing the performance of turbo-equalised bit-interleaved turbo-coded modulation," In *Proc. Symposium on Commun. Vehicular Tech.*, Ghent (Belgium), 2004.
- [26] N. Noels, H. Steendam and M. Moeneclaey, "On the Cramer-Rao lower Bound and the performance of synchronizers for (turbo) encoded systems," In *Proc. 5th IEEE Workshop Sig. Proc. Advances in Wirel. Commun.*, Lisbon, Portugal, July 11-14, 2004.
- [27] P. Robertson, P. Hoher and E. Vilebrun, "Optimal and Sub-optimal maximum a posteriori algorithms suitable for turbo decoding," In *European Trans. On Telecomm.* vol. 8, no. March/ April, pp. 119-125, 1997.

Thomas O. Olwal (M'09), obtained BSc. (1st Class Hons.) in Electrical & Electronic Engineering from the University of Nairobi, Kenya 2003, an MTech (*cum laude*) in Telecommunication from the Tshwane University of Technology (TUT) 2006, South Africa, MSc. Electronic Engineering from ESIEE-Paris 2007 and currently working on a PhD thesis with TUT and Paris-Est University, France. He works for Council for Scientific and Industrial Research (CSIR) as a researcher. His research interests are in timing recovery and energy-efficient operations for Wireless Networks.